Dynamic Vibration Absorbers for Vibration Control within a Frequency Band

Cheng YANG** Deyu LI** and Li CHENG**,^

**Department of Mechanical Engineering, The Hong Kong Polytechnic University,
Hung Hom, Kowloon, Hong Kong, SAR of China,
^E-mail: mmlcheng@polyu.edu.hk

Abstract

The use of dynamic vibration absorbers to control the vibration of a structure in both narrow and broad bands is discussed in this paper. As a benchmark problem, a plate incorporating multiple vibration absorbers is formulated, leading to an analytical solution when the number of absorbers yields to one. Using this analytical solution, control mechanisms of the vibration absorber in different frequency bandwidths are studied; the coupling properties due to the introduction of the absorber into the host structure are analyzed; and the control performance of the absorber in different control bandwidths is examined regarding to its damping and location. It is found that the interaction between the plate and the absorber by means of the reaction force from the absorber plays a dominant role in a narrow band control, while in a relatively broad band control, the dissipation by the absorber damping governs the control performance. Numerical findings are assessed based on a simply-supported plate and a fair agreement between the predicted and measured results is obtained.

Key words: dynamic vibration absorber, control mechanism

1. Introduction

Dynamic vibration absorbers (DVA) are widely used for the control of structural vibration and noise radiation. The working principle of a DVA has long been demonstrated by Ormondroyd and Den Hartog [1] using a single degree of freedom (SDOF) system. Historically, the DVA was first found its utilization in the vibration control at a single frequency, predominantly at the resonance frequency of the system [2-3]. A DVA is also used to suppress vibration over a frequency band, generally in the vicinity of a targeted frequency. For SDOF systems, the well-known fixed-point method was presented [4], and the absorber was found to be most favorably tuned when the two coupled peaks lying inside the frequency range have equal amplitude [5]. For multiple degrees of freedom (MDOF), the tuning process becomes more delicate as the absorber is coupled with all structural modes of the host systems. Free and forced vibrations of a plate with embedded DVAs were also analytically investigated in [6-8]. It was observed that the insertion of DVAs into the host structure reconstructs the contribution of modal response [9], which in turn affects the characteristics of the system and thus appeals for a proper selection of absorber parameters, such as damping and location.

It is evident that the band control capability of DVAs aroused great interest due to its practical application value. Despite the persistent effort made in the past, however, several key issues have not been fully understood. Two aspects are on the top of the list. First, the working mechanism of DVA may differ as the frequency bandwidth changes. This will impact on the tuning of the DVA parameters to achieve the optimal band control

performance. Second, both the insertion of DVAs and the enlargement of the frequency band may result in a more active coupling among structural modes, which in turn affects the optimal location of the DVAs. A good understanding of these two issues can not only help reveal the physical insight on the interaction between absorber and host system but also give guidance to the design of DVAs for practical engineering applications.

2. Theory

The system under consideration consists of a homogeneous, orthotropic and thin rectangular plate with M DVAs, as shown in Fig.1. The plate is subject to a harmonic point force of $Fe^{i\omega t}$ at (x_0, y_0).

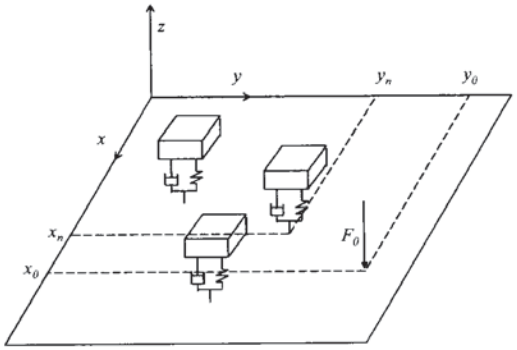

Fig. 1 A plate incorporating multiple dynamic vibration absorbers.

2.1 General coupled model of a plate with DVAs

The motion of the nth absorber follows the Newton's second law as:

$$m_n\ddot{z}_n(t)+c_n\dot{z}_n(t)+k_n z_n(t)=c_n\dot{w}(x_n,y_n,t)+k_n w(x_n,y_n,t) \tag{1}$$

where $z_n(t)$, m_n, c_n and k_n represent the displacement, mass, damping constant and stiffness of the nth absorber, respectively; $w(x_n, y_n, t)$ is the lateral displacement of the plate at the absorber location (x_n, y_n).

Under harmonic excitation at an angular frequency ω, the equation of motion for the plate is expressed as [10]

$$\begin{aligned} &D\nabla^4 w(x,y)-\omega^2\rho w(x,y)=F\delta(x-x_0)\delta(y-y_0)+\\ &\sum_{n=1}^{M}\left(\mathrm{i}\omega c_n\left[Z_n-w(x_n,y_n)\right]+k_n\left[Z_n-w(x_n,y_n)\right]\right)\delta(x-x_n)\delta(y-y_n) \end{aligned} \tag{2}$$

where D is the flexural rigidity of the plate; ρ the area density; and δ the Dirac delta function; Z_n the displacement amplitude of $z_n(t)$.

Using modal expansion method, the displacement $w(x, y)$ of the plate can be expanded on the basis of mode shapes of the plate $w(x,y)=\sum_{j=1}^{J} W_j\Phi_j(x,y)$, where W_j is the jth modal displacement, $\Phi_j(x, y)$ is the jth mode shape, and J is the maximum mode number used in computation. Making use of the orthogonality property of the mode shapes, a set of decoupled equations can be obtained from Eq. (2) as

$$\beta_j^2 W_j-\omega^2 W_j+\mathrm{i}2\omega\xi_j\beta_j W_j=F\frac{\Phi_j(x_0,y_0)}{M_j}+\omega^2\sum_{n=1}^{M}\frac{m_n}{M_j}Z_n\Phi_j(x_n,y_n),\ \left(j=1,2,\ldots J\right) \tag{3}$$

where β_j is the jth natural angular frequency, M_j is the jth modal mass, represented as $M_j=\rho\int_S\left[\Phi_j(x,y)\right]^2 dxdy$, ξ_j is the jth modal damping ratio, and S is the plate area. Notice that the term $\mathrm{i}2\omega\xi_j\beta_j W_j$ on the left hand side has been introduced to represent the damping effect of the plate.

Now substituting the modal expansion expression of the plate displacement into Eq. (1), the distance amplitude Z_n of the nth DVA is obtained as

$$Z_n = T_n \sum_{h=1}^{H} W_h \Phi_h(x_n, y_n) \tag{4}$$

where T_n is a dynamic parameter defined as

$$T_n = \frac{\omega_n^2 + \mathrm{i}2\xi_n'\omega\omega_n}{\omega_n^2 - \omega^2 + \mathrm{i}2\xi_n'\omega\omega_n}$$

where ξ_n' and ω_n are the damping ratio and the natural angular frequency of the nth DVA, respectively . Substituting Eq. (4) into Eq. (3) yields

$$\left(\left(\beta_j^2 - \omega^2 + \mathrm{i}2\xi_j\omega\beta_j\right) - \omega^2 \sum_{n=1}^{M} T_n \frac{m_n}{M_j} \Phi_j^2(x_n, y_n)\right) W_j - \omega^2 \sum_{h\neq j}^{H} \sum_{n=1}^{M} T_n \frac{m_n}{M_j} \Phi_h(x_n, y_n) \Phi_j(x_n, y_n) W_h = \frac{\Phi_j(x_0, y_0)}{M_j} F \tag{5}$$

The above equation involves J modes. It should be stated that, actually, Eq. (5) is a linear system of equations in terms of the modal response W_j. W_j can be numerically solved provided the plate mode shapes are known and detailed information of the DVAs and excitation force are given. In the absence of DVA, i.e. T_n=0, the modal amplitude is solved as

$$\left(W_j\right)_{\text{without DVA}} = \frac{1}{\beta_j^2 - \omega^2 + \mathrm{i}2\xi_j\omega\beta_j} \frac{\Phi_j(x_0, y_0)}{M_j} F \tag{6}$$

2.2 Analytical solution with a single DVA

Assuming only the nth DVA is installed on the plate, Eq. (5) is simplified to

$$\left(\beta_j^2 - \omega^2 + \mathrm{i}2\xi_j\omega\beta_j\right) W_j - \omega^2 T_n \frac{m_n}{M_j} \Phi_j(x_n, y_n) \sum_{h=1}^{H} W_h \Phi_h(x_n, y_n) = \frac{\Phi_j(x_0, y_0)}{M_j} F \tag{7}$$

Dividing $m_n / M_j \Phi_j(x_n, y_n)$ over all the terms in Eq. (7) gives

$$\frac{\left(\beta_j^2 - \omega^2 + \mathrm{i}2\xi_j\omega\beta_j\right) W_j}{\frac{m_n}{M_j} \Phi_j(x_n, y_n)} - \omega^2 T_n \sum_{h=1}^{H} W_h \Phi_h(x_n, y_n) = \frac{\Phi_j(x_0, y_0)}{\Phi_j(x_n, y_n)} \frac{F}{m_n} \tag{8}$$

Notice that the second term on the left hand side of Eq. (8) is independent of index j. Changing the running index with integer g gives another equation as

$$\frac{\left(\beta_g^2 - \omega^2 + \mathrm{i}2\xi_g\omega\beta_g\right) W_g}{\Phi_g(x_n, y_n) \frac{m_n}{M_g}} - \omega^2 T_n \sum_{h=1}^{H} W_h \Phi_h(x_n, y_n) = \frac{\Phi_g(x_0, y_0)}{\Phi_g(x_n, y_n)} \frac{F}{m_n} \tag{9}$$

Subtracting Eqs.(8) and (9) yields

$$\frac{\left(\beta_j^2 - \omega^2 + \mathrm{i}2\xi_j\omega\beta_j\right) W_j}{\Phi_j(x_n, y_n) \frac{m_n}{M_j}} - \frac{\left(\beta_g^2 - \omega^2 + \mathrm{i}2\xi_g\omega\beta_g\right) W_g}{\Phi_g(x_n, y_n) \frac{m_n}{M_g}} = \left(\frac{\Phi_j(x_0, y_0)}{\Phi_j(x_n, y_n)} - \frac{\Phi_g(x_0, y_0)}{\Phi_g(x_n, y_n)}\right) \frac{F}{m_n} \tag{10}$$

Equation (10) establishes a direct relationship between any two arbitrary plate modes, g and j. In this case, the modal response W_g can be expressed in terms of W_j, and substituting the new W_g expression into the independent term in Eq. (8) gives

$$\begin{aligned} &\frac{\beta_j^2 - \omega^2 + \mathrm{i}2\xi_j\omega\beta_j}{\Phi_j(x_n, y_n) \frac{m_n}{M_j}} \left(1 - m_n\omega^2 T_n \sum_{h=1}^{H} \frac{\Phi_h^2(x_n, y_n)}{\left(\beta_h^2 - \omega^2 + \mathrm{i}2\xi_h\omega\beta_h\right) M_h}\right) W_j = \\ &\left(1 - m_n\omega^2 T_n \sum_{h=1}^{H} \frac{\Phi_h^2(x_n, y_n)}{\left(\beta_h^2 - \omega^2 + \mathrm{i}2\xi_h\omega\beta_h\right) M_h}\right) \frac{\Phi_j(x_0, y_0)}{\Phi_j(x_n, y_n)} \frac{F}{m_n} + \\ &\omega^2 T_n \sum_{h=1}^{H} \frac{\Phi_h(x_0, y_0) \Phi_h(x_n, y_n) F}{M_h \left(\beta_h^2 - \omega^2 + \mathrm{i}2\xi_h\omega\beta_h\right)} \end{aligned} \tag{11}$$

Therefore, an analytical solution of W_j is obtained from Eq. (11) as

$$W_j = \underbrace{\frac{1}{\beta_j^2 - \omega^2 + \mathrm{i}2\xi_j\omega\beta_j}\frac{\Phi_j(x_0,y_0)}{M_j}F}_{\text{Contribution from the primary force}} + \underbrace{\frac{1}{\beta_j^2 - \omega^2 + \mathrm{i}2\xi_j\omega\beta_j}\frac{\Phi_j(x_n,y_n)}{M_j}F_{\text{second}}}_{\text{Contribution from the DVA}} \tag{12}$$

where

$$F_{\text{second}} = \frac{m_n\omega^2 T_n \sum_{h=1}^{H}\frac{\Phi_h(x_0,y_0)\Phi_h(x_n,y_n)F}{M_h\left(\beta_h^2 - \omega^2 + \mathrm{i}2\xi_h\omega\beta_h\right)}}{1 - m_n\omega^2 T_n \sum_{h=1}^{H}\frac{\Phi_h^2(x_n,y_n)}{M_h\left(\beta_h^2 - \omega^2 + \mathrm{i}2\xi_h\omega\beta_h\right)}} \tag{13}$$

Equation (12) clearly shows that the modal amplitude is composed of two parts: one is the effect induced by the primary exciting force (first term) and the second part comes from the reaction force by the DVA (second term). It is also seen in Eq. (13) that the absorber is coupled with all plate modes. This fully coupled term F_{second} represents the reaction force of the DVA on the plate. It is noted that Eq. (7) and its analytical solution Eq. (12) can be applied to the situation in which there are M identical DVAs attached at the same place (x_n, y_n), but each DVA has only $1/M$ mass of m_n.

Assuming only one targeted mode i.e. the jth mode, dominates the response, Eq. (12) can be expressed in a dimensionless form as

$$Q = \frac{W_j}{\left(W_j\right)_{\text{without DVA}}} = \frac{1}{1 - \dfrac{\mu_{nj}\omega^2 T_n \Phi_j^2(x_n,y_n)}{\beta_j^2 - \omega^2 + \mathrm{i}2\xi_j\omega\beta_j}} \tag{14}$$

where μ_{nj} is the ratio of the nth absorber mass to the jth modal mass of plate. It can be seen from Eq. (14) that the Q depends on its dynamic parameter T_n and the absorber mass ratio μ_{nj}. As an extreme case, if the attachment is made at the node of the jth mode, i.e. $\Phi_h(x_n, y_n)=0$, the reacting force becomes 'contributiveless' to the modal displacement at this mode.

2.3 Qualification of the control performance

To assess the performance of the DVA, an 'energy reduction index' is defined as

$$E_r = 10\log_{10}\frac{E_b^0}{E_b^1} \tag{15}$$

where E_b^1 and E_b^0 are averaged kinetic energy of the plate within a chosen bandwidth [ω_1, ω_2] with and without DVAs, respectively. The following expression can be used to calculate the averaged kinetic energy E_b:

$$E_b = \int_{\omega_1}^{\omega_2}\frac{1}{2}M\left\langle V^2\right\rangle d\omega \tag{16}$$

where M is the mass of the plate, and $\langle V^2\rangle$ is the averaged quadratic velocity of the plate, which is computed by

$$\left\langle V^2\right\rangle = \frac{\omega^2}{S}\int_S w(x,y)w^*(x,y)\,dxdy \tag{17}$$

where the asterisk denotes complex conjugate.

The energy dissipated by the DVA damping in one period T can be calculated by

$$E_d = \frac{1}{2}\int_0^T c_n\omega^2\left|z_n(t) - w(x_n,y_n,t)\right|^2 dt \tag{18}$$

where $[z_n(t)-w(x_n, y_n, t)]$ is the relative displacement between the plate and the DVA at the attaching point.

For the harmonic motion, Eq. (18) is simplified as

$$E_d = \frac{1}{4} T c_n \omega^2 \left| Z_n - w(x_n, y_n) \right|^2 \tag{19}$$

The work done by the reacting force within the bandwidth is calculated by

$$E_f = \int_{\omega_1}^{\omega_2} \frac{1}{2} k_n \left| Z_n - w(x_n, y_n) \right|^2 d\omega \tag{20}$$

3. Control mechanism and coupling analysis in different frequency bandwidths

A simply-supported aluminum plate as shown in Fig. 2(a), having a dimension of 0.41×0.45×0.003 m, is used. A primary excitation point force is exerted at (0.28 m, 0.38 m). The frequency response function (FRF) of the plate observed at (0.17 m, 0.20 m) is plotted in Fig. 2 (b). It can be seen that the first mode (1, 1) at 85 Hz is well-separated from all other modes, while the second mode (1, 2) at 200 Hz has a close neighboring mode (2, 1) at 224 Hz. The second and the third modes close each other, they are denoted as a closely-packed mode pair. Both of these two kinds of modes (well-separated mode and closely-packed mode) are examined in the following study.

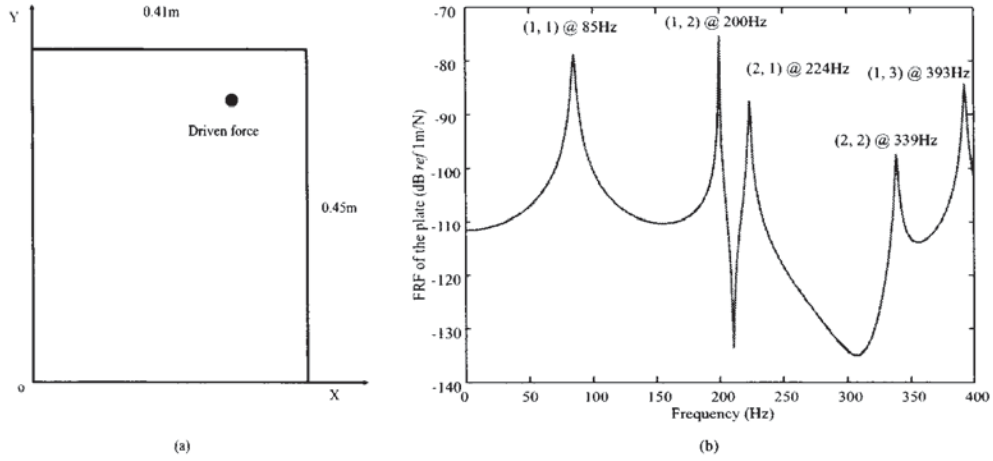

Fig. 2 (a) Coordinate system of the plate, (b) predicted FRF of the plate at (0.17m, 0.20m) without DVA.

3.1 Control mechanism of DVA for different bandwidths

The FRF of the plate centered at 85 Hz with and without a DVA are calculated at an arbitrary point of (0.17 m, 0.20 m). The absorber is tuned at the resonance 85 Hz and the mass is set as 1% of the plate, i.e. 0.015 kg. DVAs with three typical damping values (ξ=0.012, 0.041, and 0.088) are compared to show the effect of the damping on the control performance. It can be seen from Fig. 3 that for ξ=0.012, although the reduction is significant at the central frequency of 85 Hz, a pair of new peaks appear. Judging from the peak values within the bandwidth, only a reduction of 4.2 dB is achieved. Increasing the damping ratio to the optimal one, i.e. ξ=0.041, these two new peaks are smoothed down. By further increasing the damping ratio to ξ=0.088, the two coupled peaks disappear to form a single peak. Obviously, the lightly-damped absorber can perfectly suppress the vibration only at the resonance frequency. If a wide frequency band is considered, however, the control mechanism would be different. In this case, a proper balance between the absorber damping and the selected bandwidth is needed.

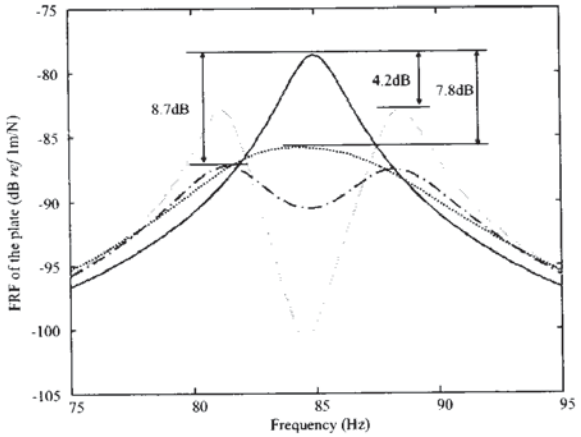

Fig. 3 Effect of the absorber damping on the FRF of the plate observed at (0.17m, 0.20m). ——, without DVA; — —, ξ=0.012; — • —, ξ=0.041; ••••, ξ=0.088.

The control mechanism of the DVA is first investigated by choosing a bandwidth of 20 Hz centered at 85 Hz. The energy reduction of the plate, the dissipation energy by the DVA, and the work done by the reacting force are calculated using Eqs. (15), (19) and (20) for different DVA damping ratios. Results are shown in Fig. 4(a-c). In Fig. 4(a) at low damping, the increase of damping benefits the energy reduction E_r of the host structure, and a maximum reduction is reached when the damping ration is ξ = 0.041. After that, the increase of damping weakens the energy reduction. A similar trend is observed in the bandwidth energy dissipation E_d of the DVA, as illustrated in Fig. 4(b). The tendency match between E_d and E_r suggests that in a relatively large bandwidth, e.g. 20Hz, the energy reduction of the host system is dominated by the dissipation of DVA. But a threshold exists beyond which no further energy reduction can be achieved. Figure 4(c) also suggests a strong coupling between the absorber and plate at low damping, as evidenced by the efficient energy feedback to the plate. Excessive damping, however, reduces the motion of the absorber and therefore influences the energy transmission between the DVA and the plate, which consequently constrains the energy dissipation as well.

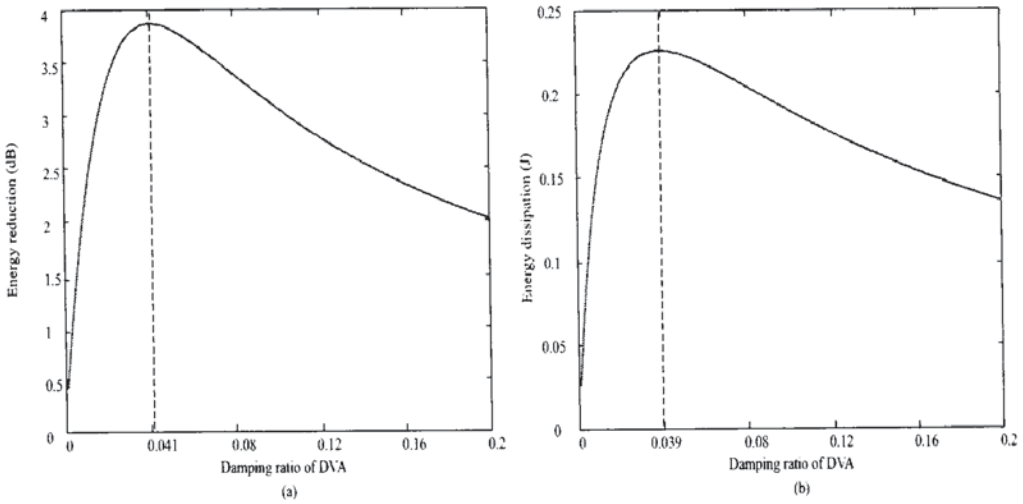

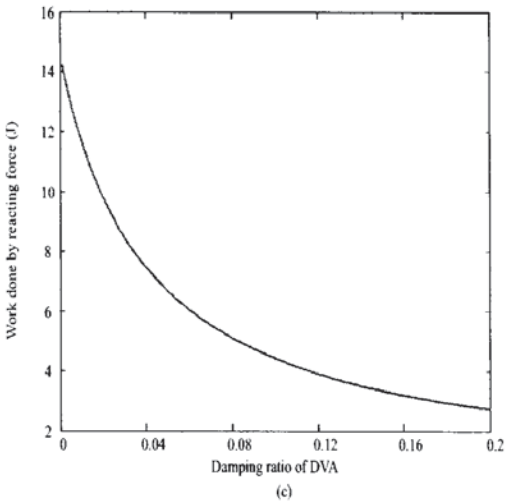

Fig. 4 Dependence of energy terms on damping ratios of the absorber in 20 Hz bandwidth. (a) Energy reduction of plate, (b) energy dissipation by DVA, (c) work done by reacting force.

It is expected that the aforementioned control mechanism only applies when the frequency band of interest is relatively large. The damping ratio of DVA is determined in two different ways: 1) the damping corresponding to the maximum energy reduction of the plate is defined as the optimal damping, indicated by ξ_{red}; and 2) the damping corresponding to the maximum energy dissipation of the absorber denoted by ξ_{dis}. The variations of ξ_{red} and ξ_{dis} against the frequency bandwidth are illustrated in Fig. 5. It is observed that when the frequency bandwidth is very small, the damping ratios determined by the above two methods has a significant difference. As the bandwidth increase, the two damping ratios get closer.

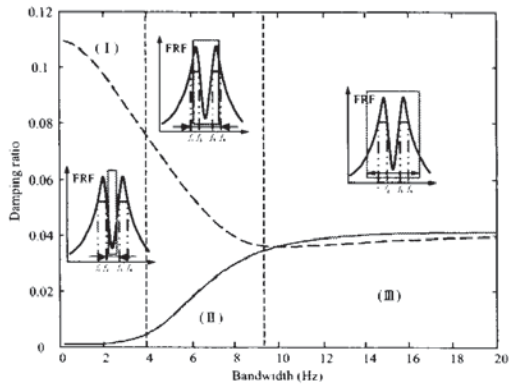

Fig. 5 Optimal damping ratio v.s. bandwidth: ——, optimal damping ratio ξred from maximum energy reduction of plate; — —, damping ratio ξdis from maximum energy dissipation of DVA.

3.2 Coupling analysis in terms of bandwidths and DVA locations

To qualify the coupling effect, a bandwidth energy variation parameter EV is defined as

$$\mathrm{EV} = 10\log_{10}\left(\int_{\omega_1}^{\omega_2} \frac{E_b^0}{E_b^j}\, d\omega\right) \tag{21}$$

where E_b^0 is the bandwidth averaged kinetic energies of the plate when a converged solution is obtained using 400 modes, and E_b^j is the bandwidth averaged kinetic energies of the plate when the first j modes are considered in computation. For a 20 Hz bandwidth centered at 200 Hz, the EVs before and after installing the DVA are shown in Fig. 6. It can be seen that, in the absence of absorber, EV converges very rapidly since only a few modes contribute significantly to the response. After installing the absorber, however, more modes come into play. Participation of each individual mode can be better illustrated by

decomposing the response of the plate into each mode. To that end, the normalized modal response of the first 20 modes is shown in Fig.7. It is obvious that the presence of DVA activates more plate modes such (2, 1), (2, 2) and (2, 3).

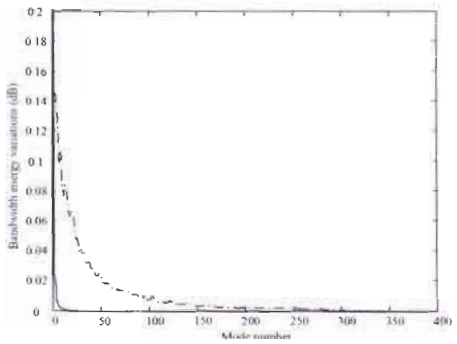

Fig. 6 20 Hz bandwidth energy variations v.s. number of plate modes before and after installing DVA. ——, without absorber; — • —, with absorber.

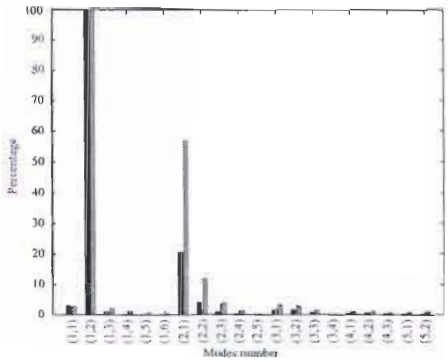

Fig. 7 Contribution percentage of each mode against the maximum mode. Dark bars, without DVA; Light bars, with DVA.

4. Experimental validations

Measurements are conducted to validate the results presented above. In Fig. 8(a), a simply supported aluminum plate, having the same dimension as in simulation, is fabricated and installed on an isolation table. A single point primary force is applied at (0.28m, 0.38m) using a Brüel & Kjær Type 4809 shaker. Vibrations are measured using a PSV-400 Scanning Laser-vibrometer. The measured and computed FRF curves of the plate at location (0.123 m, 0.113 m) are compared in Fig. 9. The good match between the measured and predicted curves in the frequency range of interest shows that the simply-supported boundary conditions of the plate used in the experiment is well satisfied.

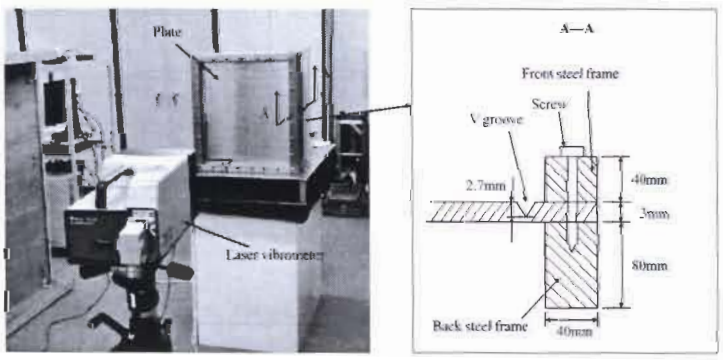

(a)

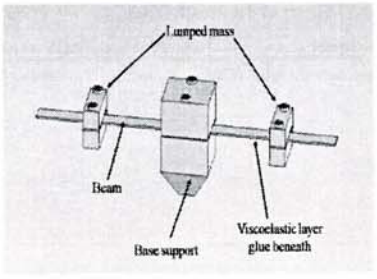

(b)

Fig. 8 Experimental set up. (a) Test bed, (b) beam-mass type DVA.

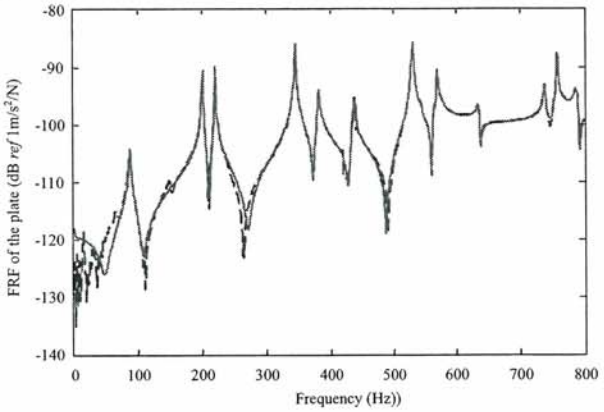

Fig. 9 FRF curves of the plate observed at (0.123 m, 0.113 m) without DVAs. ——, Predicted result; — —, Measured result.

The DVA is designed and fabricated using two identical back to back beam-mass elements, symmetrically arranged with respect to the central axis (Fig. 8(b)). The damping ratio of the absorbers was tuned by applying a damping layer coated on the surface of the beam. The vibration control at the first resonance of 85 Hz using the DVA is carried out. The FRF of the plate with an absorber is measured at (0.17 m, 0.20 m) and shown in Fig. 10. Similar to the simulation in Fig. 3, the beam-mass absorbers are designed to have three typical damping ratios. Due to the practical difficulty in getting exactly the desired optimal damping value, (ξ_{red}=0.041), the best achieved damping used in the experiment is ξ=0.039 which is near the optimal result. With this damping, a 6.8 dB reduction is achieved, which is 1 dB smaller than the predicted result. For the small and large damping, the two sharp peaks and the single peak occur, respectively, consistent with numerical predictions. In general, the control performance of each absorber agrees with the numerical results to an acceptable extent and the optimal damping obtained is capable to provide the highest reduction.

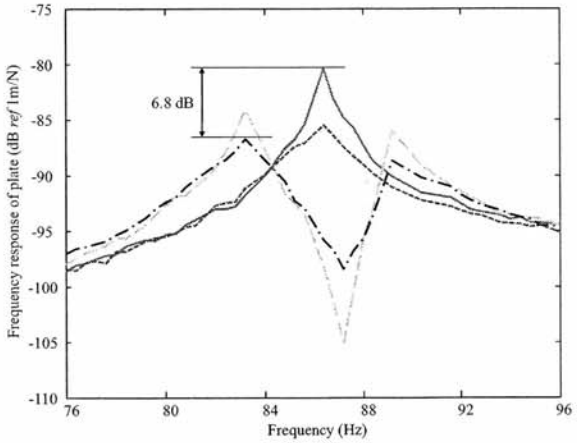

Fig. 10 Measured FRF curves of the plate observed at (0.17 m, 0.20 m). ——, without DVA; — —, ξ=0.012; — • —, ξ=0.088; ••••, ξ=0.039.

5. Conclusions

In this paper, a dynamic vibration absorber is used to suppress the vibration of a plate in a frequency band. The control mechanism is investigated with respect to different bandwidth, and the coupling is also examined in terms of the frequency bandwidth. By means of a mathematical model, it is found that the control mechanism of the DVA depends on the frequency bandwidth: for a narrow band control, the interaction between the DVA and the host structure by means of the reacting force from the absorber dominates the control performance; as the bandwidth gradually increases, there is a growing importance of energy dissipation; for a relatively wide band control, the energy dissipation of the DVA becomes a dominant factor.

References

(1) J. Ormondroyd, J.P. Den Hartog, The theory of dynamic vibration absorber, Journal of Applied Mechanics, Volume 50, 1928, pp. 9-22.

(2) D. Young, Theory of dynamic vibration absorbers for beams, Proceedings of the First U. S. National Congress of Applied Mechanics, New York, 1952, pp. 91-96.

(3) J. C. Snowdon, Vibration of cantilever beams to which dynamic absorbers are attached, Journal of Acoustical Society of America, Volume 39, 1966, pp. 878-886.

(4) J. P. Den Hartog, Mechanical vibration, McGraw-Hill, New York, 1956.

(5) J. C. Snowdon, Vibration and shock in damped mechanical systems, John Wiley & Sons, New York, 1968.

(6) R. G. Jacquot and W. Soedel, Vibrations of elastic surface systems carrying dynamic elements, Journal of Acoustical Society of America, Volume 47, 1970, pp. 1354-1358.

(7) R. G. Jacquot, The forced vibration of singly modified damped elastic surface systems, Journal of Sound and Vibration, Volume 48, 1976, pp. 195-201.

(8) J. W. Nicholson and L. A. Bergman, Vibration of damped plate-oscillator systems, Journal of Engineering Mechanics, Volume 112, 1986, pp. 14-30.

(9) C. R. Fuller, J. P. Mailard, M. Mercadal, and A. H. von Flotow, Control of aircraft interior noise using globally detuned vibration absorbers, Journal of Sound and Vibration, Volume 203, 1997, pp. 745-761.

(10) R. G. Jacquot, Suppression of random vibration in plates using vibration absorbers, Journal of Sound and Vibration, Volume 248, 2001, pp. 585-596.

Acknowledgements

The authors wish to acknowledge support given to them by the Research Grants Council of HKSAR through Grant No. PolyU 5140/09E.